

# Advanced spectroscopic investigation of colour centres in LiF crystals irradiated with monochromatic hard x-rays

M A Vincenti<sup>1,\*</sup> , R M Montereali<sup>1</sup> , F Bonfigli<sup>1</sup>, E Nichelatti<sup>2</sup>, V Nigro<sup>1</sup> , M Piccinini<sup>1</sup>, M Koenig<sup>3</sup>, P Mabey<sup>4</sup>, G Rigon<sup>3,5</sup>, H J Dabrowski<sup>3</sup>, Y Benkadoum<sup>3</sup>, P Mercere<sup>6</sup>, P Da Silva<sup>6</sup>, T Pikuz<sup>7</sup>, N Ozaki<sup>8</sup>, S Makarov<sup>9</sup>, S Pikuz<sup>9</sup> and B Albertazzi<sup>3</sup>

<sup>1</sup> Fusion and Technologies for Nuclear Safety and Security Department, ENEA C.R. Frascati, Rome, Italy

<sup>2</sup> Fusion and Technologies for Nuclear Safety and Security Department, ENEA C.R. Casaccia, Rome, Italy

<sup>3</sup> LULI-CNRS, Ecole Polytechnique, CEA, Université Paris-Saclay, Palaiseau Cedex, France

<sup>4</sup> Department of Physics, Freie Universität Berlin, Berlin, Germany

<sup>5</sup> Massachusetts Institute of Technology, Cambridge, MA, United States of America

<sup>6</sup> SOLEIL synchrotron, L'Orme des Merisiers, Départementale 128, Saint Aubin, France

<sup>7</sup> Institute for Open and Transdisciplinary Research Initiatives, Osaka University, Osaka, Japan

<sup>8</sup> Graduate School of Engineering, Osaka University, Osaka, Japan

<sup>9</sup> Joint Institute for High Temperature RAS, Moscow, Russia

E-mail: [aurora.vincenti@enea.it](mailto:aurora.vincenti@enea.it)

Received 31 October 2023, revised 30 January 2024

Accepted for publication 8 February 2024

Published 16 February 2024



## Abstract

Nominally-pure lithium fluoride (LiF) crystals were irradiated with monochromatic hard x-rays of energy 5, 7, 9 and 12 keV at the METROLOGIE beamline of the SOLEIL synchrotron facility, in order to understand the role of the selected x-ray energy on their visible photoluminescence (PL) response, which is used for high spatial resolution 2D x-ray imaging detectors characterized by a wide dynamic range. At the energies of 7 and 12 keV the irradiations were performed at five different doses corresponding to five uniformly irradiated areas, while at 5 and 9 keV only two irradiations at two different doses were carried out. The doses were planned in a range between 4 and  $1.4 \times 10^3$  Gy ( $10.5 \text{ mJ cm}^{-3}$  to  $3.7 \text{ J cm}^{-3}$ ), depending on the x-ray energy. After irradiation at the energies of 7 and 12 keV, the spectrally-integrated visible PL intensity of the  $F_2$  and  $F_3^+$  colour centres (CCs) generated in the LiF crystals, carefully measured by fluorescence microscopy under blue excitation, exhibits a linear dependence on the irradiation dose in the investigated dose range. This linear behaviour was confirmed by the optical absorption spectra of the irradiated spots, which shows a similar linear behaviour for both the  $F_2$  and  $F_3^+$  CCs, as derived from their overlapping absorption band at around 450 nm. At the highest x-ray energy, the average concentrations of the

\* Author to whom any correspondence should be addressed.



Original content from this work may be used under the terms of the [Creative Commons Attribution 4.0 licence](https://creativecommons.org/licenses/by/4.0/). Any further distribution of this work must maintain attribution to the author(s) and the title of the work, journal citation and DOI.

radiation-induced  $F$ ,  $F_2$  and  $F_3^+$  CCs were also estimated. The volume distributions of  $F_2$  defects in the crystals irradiated with 5 and 9 keV x-rays were reconstructed in 3D by measuring their PL signal using a confocal laser scanning microscope operating in fluorescence mode. On-going investigations are focusing on the results obtained through this  $z$ -scanning technique to explore the potential impact of absorption effects at the excitation laser wavelength.

Keywords: lithium fluoride, colour centres, photoluminescence, monochromatic hard x-rays

## 1. Introduction

X-ray diagnostic techniques characterised by high spatial resolution such as x-ray microscopy, micro-radiography, diffraction and phase-contrast imaging are extensively used in various experimental fields ranging from medicine to material science [1, 2]. Development of these techniques requires the use of x-ray detectors with excellent performances in terms of spatial resolution, dynamic range, field of view and non-destructive readout capabilities [3]. In recent years, passive solid-state detectors based on colour centres (CCs) photoluminescence (PL) in lithium fluoride (LiF) crystals and thin films have been proposed and successfully tested for 2D x-ray imaging [4–7] and hard x-rays free electron laser diagnostics [3, 8, 9], including 3D visualization of the focused beam and its energy distribution, which is still challenge. These radiation imaging detectors are characterised by high intrinsic spatial resolution over a large field of view, wide dynamic range and simplicity of use as they are insensitive to ambient light and do not require any processing after irradiation [10, 11]. Moreover, they are reusable after proper thermal annealing. Their principle of operation is the optical reading of visible PL emitted by the  $F_2$  and  $F_3^+$  CCs, locally-induced by radiation, which are stable at room temperature (RT) [12, 13]. The primary electronic defect induced by irradiation is the  $F$  centre, which consists of an anionic vacancy binding an electron. The primary absorption band due to  $F$  centres, named  $F$  absorption band, is located at a wavelength of about 248 nm [14]. Although PL from  $F$  centres was investigated since long time [12, 15] and a weak emission is theoretically expected around 900 nm, it was not detected unambiguously up to now [16–18], as it should be superimposed on the emission band of the  $F_2^+$  centres [19, 20]. The aggregate laser-active  $F_2$  and  $F_3^+$  CCs (two and three anion vacancies binding two electrons, respectively) possess almost overlapped absorption bands peaked at about 444 and 448 nm, respectively. These absorption bands together form the so called broad M band in LiF [19]. Under optical pumping in this spectral region, the  $F_2$  and  $F_3^+$  CCs simultaneously emit visible PL in broad bands, peaked at 678 nm and 541 nm, respectively [19, 21]. Their spectrally-integrated PL can be read in non-destructive way by using conventional and confocal fluorescence microscopy.

In this study, we report and discuss experimental results concerning the optical behaviour of LiF crystals irradiated with monochromatic x-rays of energy 5, 7, 9 and 12 keV at several doses in the range between 4 and  $1.4 \times 10^3$  Gy to investigate the possibility to extend their use to 3D imaging.

## 2. Materials and methods

Three commercially-available nominally-pure polished LiF crystals, each circular with a diameter of 20 mm and a thickness of 2 mm, were irradiated with monochromatic x-rays at the METROLOGIE beamline of the SOLEIL synchrotron facility (Paris, France). The LiF crystals were mounted on a specially-designed sample holder, motorised in the  $xyz$  directions. The incident photon flux was measured, both before and after each irradiation, using a diode placed in the same plane as the LiF samples. By using the measured values of photon flux, depending on the x-ray energy and attenuation length,  $L$  [22], the energy depth distribution was simulated and integrated along the entire crystal thickness, whose values were used to obtain the average doses reported in table 1. At the energies of 7 and 12 keV the irradiations were conducted at five different doses, corresponding to five distinct uniformly irradiated areas (spots), while at 5 and 9 keV only two irradiations at two different doses were performed (two spots for each energy).

X-ray irradiation of LiF crystals enables the storage of a ‘volumetric information’ through the local generation of spatially distributed CCs along a depth in the crystal that depends on the photon energy. In table 1, the theoretical x-ray attenuation length in LiF [22],  $L$ , defined as the depth into the material where the intensity of x-rays falls to  $1/e$  of its value at the surface, is reported for each energy value.

The visible PL signal emitted from the irradiated spots of the LiF crystals under blue light excitation was examined using an optical microscope (Nikon Eclipse 80i) operating in fluorescence mode. This microscope is equipped with an excitation source consisting of a properly-filtered 100 W mercury lamp and an Andor Neo s-CMOS camera (16 bit, cooled at  $-30^\circ\text{C}$ ) as imaging detector.

Using the same microscope, operating as a confocal laser scanning microscope (CLSM) with a 445 nm continuous-wave laser for excitation and a detection system comprising two optically filtered photomultipliers, the 3D PL intensity depth distributions due to the generated  $F_2$  CCs were acquired. Indeed, by scanning along the depth ( $z$  optical axis), the CLSM operates an optical sectioning of the observed sample, detecting the PL signal only from the in-focus planes. Starting from these acquisitions, 3D reconstructions of the PL signal emitted by  $F_2$  defects were obtained with the microscope software.

Optical absorption spectra of the irradiated spots, measured at RT in a Perkin Elmer Lambda 1050+ spectrophotometer, allowed to investigate the formation of primary and aggregate

**Table 1.** X-ray irradiation dose delivered to the three LiF crystals at the beam energy of 5, 7, 9 and 12 keV, and corresponding x-ray attenuation lengths  $L$  in LiF [22].

Sample	Beam energy (keV)	$L$ ( $\mu\text{m}$ )	Average dose (Gy)
LiF1	5	78.8	$24.928 \pm 0.006$
			$246.2 \pm 0.5$
	9	475.0	$22.24 \pm 0.04$ $221.5 \pm 0.6$
LiF2	7	222.1	$20.1637 \pm 0.0005$
			$38.8 \pm 0.1$
			$186 \pm 3$
			$382 \pm 2$ $(1.38 \pm 0.48) \times 10^3$
LiF3	12	1082.0	$3.58 \pm 0.01$
			$7.19 \pm 0.03$
			$32.8 \pm 0.5$
			$259 \pm 62$
			$279 \pm 111$

defects and an estimate of the average concentrations of  $F$ ,  $F_2$ , and  $F_3^+$  CCs as functions of the irradiation dose.

### 3. Results and discussion

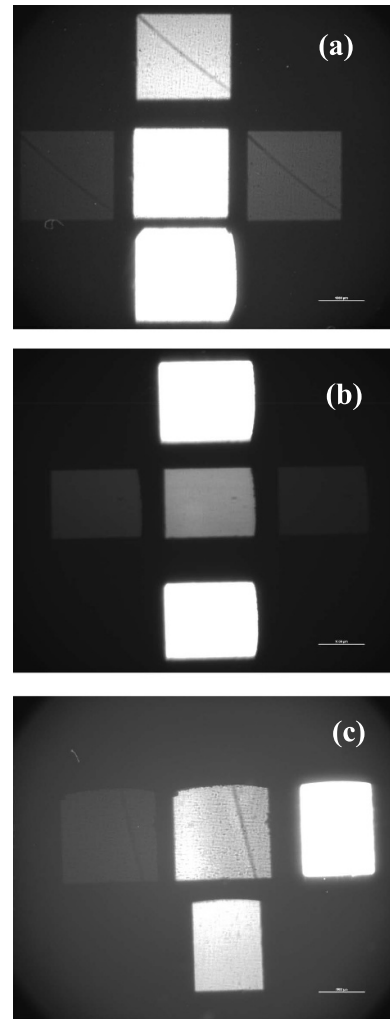
Figure 1 shows fluorescence images of coloured spots on the LiF crystals irradiated with monochromatic x-rays at 7 (a), 12 (b) and 5 and 9 (c) keV.

For each energy value, a spectrally-integrated PL intensity profile for all the irradiated spots was obtained elaborating the acquired fluorescence images using the microscope software. The net PL signal was obtained by subtracting the minimum detected PL intensity (background noise) from the measurements.

Figure 2 shows the PL intensity versus dose obtained from all the irradiated spots for each beam energy, together with linear best fits at the energies of 7 and 12 keV. For both these energies, the fits demonstrate that the PL intensity depends linearly on the irradiation dose in the investigated dose range. In figure 2, the extensive error bar linked to the data at the highest dose of 7 keV results from a significant fluctuation in beam flux that occurred during the long irradiation period.

This result is confirmed by the careful analysis of the optical absorption measurements. Figure 3 reports, as an example, the absorption spectra in optical density, OD, of the LiF crystal irradiated at five different doses with 7 keV x-rays (sample LiF2 in table 1). To highlight the effects of the colouration, the measured OD of a non-irradiated area of the same LiF crystal was subtracted from the spectra.

In each spectrum, the F absorption band due to the primary CCs and the M absorption band formed by the overlap of the  $F_2$  and  $F_3^+$  contributions are detected. Using the absorption coefficient at the band peak and the band full width at half maximum (FWHM), one can evaluate the average concentration of a given kind of CCs by applying Smakula's formula [12]. For the F band, a best-fit procedure with a Gaussian fit function and free parameters was used. The evaluation of the

**Figure 1.** Fluorescence images of the LiF crystals irradiated with monochromatic x-rays at the energies of 7 (a), 12 (b) and 5 and 9 (c) keV, acquired using the optical microscope (objective magnification 2 $\times$ , numerical aperture = 0.10, image field size  $1.67 \times 1.41$  cm $^2$ ).

same parameters for the  $F_2$  and  $F_3^+$  single contributions to the M absorption bands required a similar best fit procedure with two Gaussian functions and fixed FWHM values, following an approach reported in the literature [21].

Figure 4(a) displays the OD peak intensity of the F absorption band as functions of the average dose at the different x-ray energies. By the allometric best fits with the function  $OD = A \times Dose^b$  a value of the  $b$  parameter of  $0.71 \pm 0.01$  and  $0.65 \pm 0.11$  for 7 and 12 keV respectively, was obtained. They are very similar and in good agreement with the literature [23, 24]. Figure 4(b) reports the OD peak intensity of the M absorption band as functions of the average dose, together with the linear best fits at 7 and 12 keV. Their behaviour is similar to those obtained for PL in figure 2: the spectrally-integrated visible PL is proportional to the concentration of emitting CCs, which, in turn, is proportional to the M band absorption, at least for CCs concentration values below saturation, for which PL quenching effects do not take place. Figure 5 reports the average concentrations of F,  $F_2$  and  $F_3^+$  CCs as functions of the average dose at the energy of 12 keV, together with the

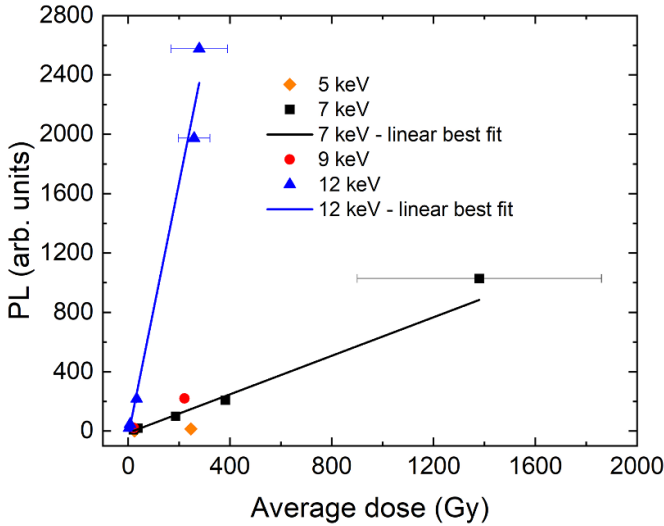


**Figure 2.** LiF crystals PL intensity response at each x-ray beam energy, together with linear best fits at the energies of 7 and 12 keV.

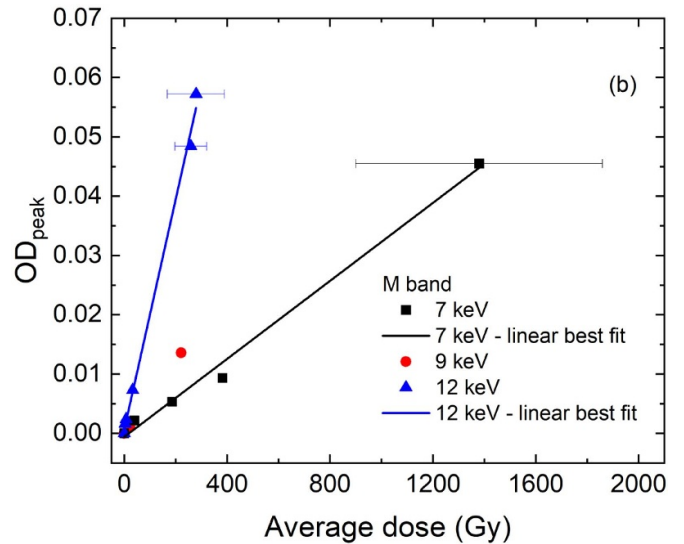
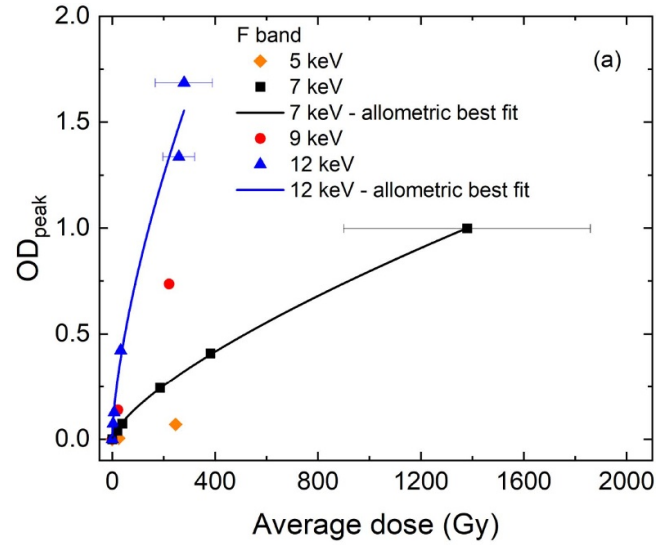


**Figure 4.** (a) OD peak intensity of the F absorption band as a function of the average dose for the LiF crystals irradiated with x-rays at the different energies. For the energies of 7 and 12 keV, their allometric best fits are plotted; (b) OD peak intensity of the M absorption band as a function of the average dose, together with linear best fits at 7 and 12 keV.

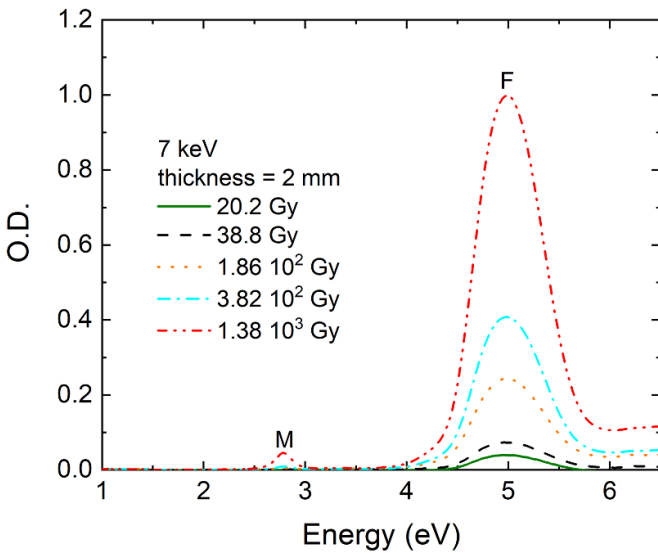


**Figure 3.** Optical absorption spectra, in OD, of the LiF crystal LiF2 irradiated at five different doses with 7 keV x-rays.

allometric best fit for the F centres and the linear best fits for the  $F_2$  and  $F_3^+$  defects. The F-colouring curve shows a rapid growing at the initial stage followed by an essentially flat region. To explain this behaviour simple kinetic models, based on the trapping of free interstitials as a channel for the stabilization of the F centres, are generally used [24]. They lead to a quasi-exponential dependence of F centre concentration on dose in agreement with the experimental data shown in figure 5, according to which the maximum concentration of primary F centre is well below  $10^{18} \text{ cm}^{-3}$ . It is confirmed that the concentration of  $F_2$  emitting defects is well below the saturation. Moreover, the volume densities of  $F_3^+$  CCs is lower than the  $F_2$  ones, as expected for irradiation at RT [16].

Figure 6 shows the 3D reconstructions of the  $F_2$  CC PL volume distributions in LiF crystals irradiated on uniform areas at 5 keV with a dose of 246.2 Gy (a) and at 9 keV with

a dose of 221.5 Gy (b). The corresponding  $xz$  slices extracted from these 3D reconstructions are reported in figures 6(c) and (d) together with the PL intensity profiles obtained along the  $z$  direction (LiF crystal thickness) (e). According to the x-ray transmission properties in solids [22], the energy deposition of x-rays decreases exponentially along the penetration depth in LiF. Assuming the CC concentrations to be proportional to the deposited energy, the confocal fluorescence microscopy is an appropriate technique to investigate their depth distributions.

In both the 3D fluorescence images, the acquired PL signal decreases with depth inside the LiF crystal. At these x-ray energies, the maximum coloration depth is well below the crystal thickness and the PL signal is negligible at the highest

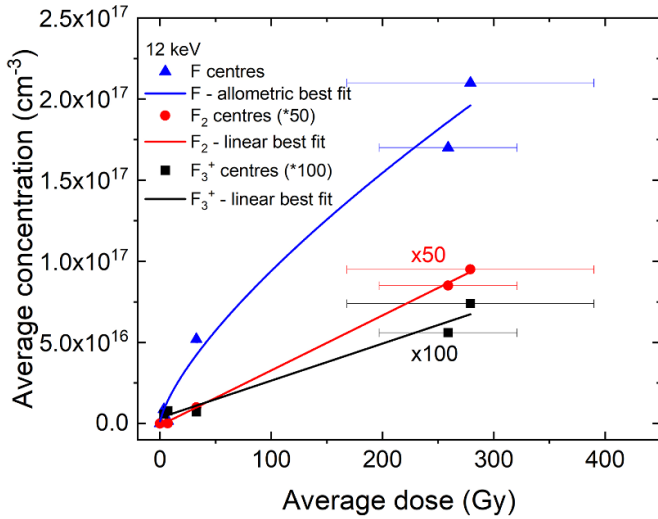


**Figure 5.** Average concentrations of F, F<sub>2</sub> and F<sub>3</sub><sup>+</sup> CCs as functions of the average dose at the energy of 12 keV, together with the allometric best fit for the F centres and the linear best fits for the F<sub>2</sub> and F<sub>3</sub><sup>+</sup> defects.

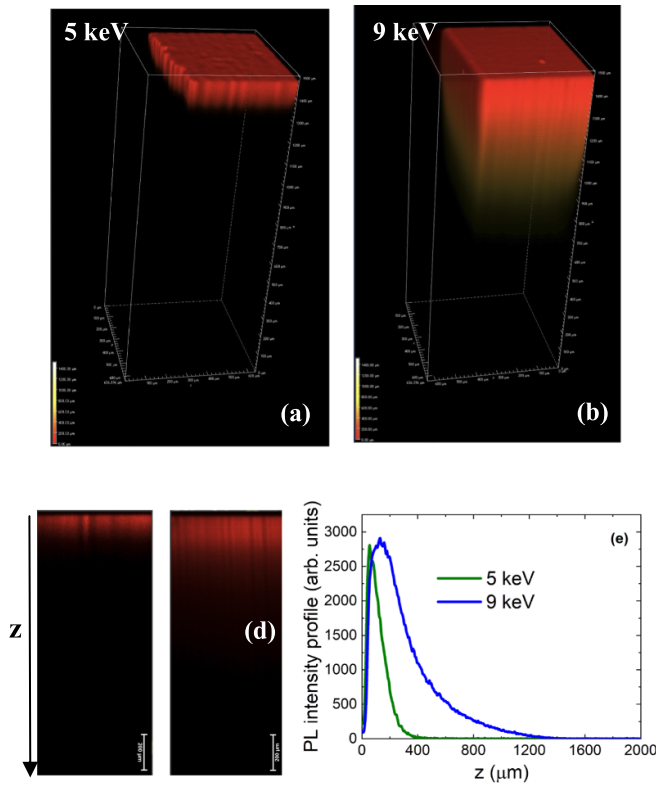


**Figure 6.** 3D reconstructions at the CLSM of x-ray-induced F<sub>2</sub> CC PL volume distributions ( $636 \times 636 \times 1500 \mu\text{m}^3$ ) in LiF crystals irradiated on uniform areas at 5 keV with a dose of 246.2 Gy (a) and at 9 keV with a dose of 221.5 Gy (b);  $xz$  slices extracted from the 3D reconstructions (c), (d); PL intensity profiles along the penetration depth  $z$  as obtained from the two  $xz$  slices (e).

depths. However, the x-ray colouration depth is only about three times higher at the energy of 9 keV than at 5 keV, which is not consistent with the values of attenuation lengths reported

in table 1. Moreover, an energy dependent rising of the PL signal is observed at the LiF-air interface. This behaviour cannot be described with a simple decreasing exponential law [25] and further investigations are under way to clarify the role of the irradiated surface and re-absorption phenomena at the laser excitation wavelength.

#### 4. Conclusions

The optical behaviour of passive LiF crystals radiation imaging detectors irradiated with monochromatic x-rays of energy 5, 7, 9 and 12 keV at different doses in the range from 4 to  $1.4 \times 10^3$  Gy was investigated. At 7 and 12 keV, the spectrally-integrated visible PL response of F<sub>2</sub> and F<sub>3</sub><sup>+</sup> defects, carefully investigated by fluorescence microscopy, shows a linear dependence on the irradiation dose. This behaviour is ascribed to a linear dependence of the volume concentrations of both these light-emitting aggregate CCs vs dose in the investigated conditions, as derived independently from the analysis of the optical absorption spectra, which allow an evaluation of the average volume concentration of F, F<sub>2</sub> and F<sub>3</sub><sup>+</sup> defects. Using a CLSM, the 3D reconstructions of x-ray-induced F<sub>2</sub> CCs PL distributions in the LiF crystals were obtained. Depending on dose and energy, further investigations are in progress to calculate the effects due to the possible absorption of the excitation laser at 445 nm, on the maximum of the M absorption band, as well as the reabsorption of the PL emitted by the CCs during  $z$ -scanning measurements in order to extend the use of LiF crystal to 3D x-ray imaging.

#### Data availability statement

All data that support the findings of this study are included within the article (and any supplementary files).

#### Acknowledgments

Research partially carried out within the TecHea (Technologies for Health) project, funded by ENEA, Italy and partially supported by KAKENHI (Grant No. 17K05729) from the Japan Society for the Promotion of Science (JSPS).

#### ORCID iDs

M A Vincenti <https://orcid.org/0000-0002-6229-4898>  
 R M Montereali <https://orcid.org/0000-0002-5540-3363>  
 V Nigro <https://orcid.org/0000-0003-0389-9982>

#### References

- [1] Endrizzi M 2018 *Nucl. Instrum. Methods Phys. Res. A* **878** 88–98
- [2] Mayo S C, Stevenson A W and Wilkins S W 2012 *Materials* **5** 937–65
- [3] Faenov A et al 2018 *Sci. Rep.* **8** 16407
- [4] Bateni S H, Bonfigli F, Cecilia A, Baumbach T, Pelliccia D, Somma F, Vincenti M A and Montereali R M 2013 *Nucl. Instrum. Methods Phys. Res. A* **720** 109–12

- [5] Baldacchini G, Bonfigli F, Faenov A, Flora F, Montereali R M, Pace A, Pikuz T and Reale L 2003 *J. Nanosci. Nanotechnol.* **3** 483–6
- [6] Bonfigli F et al 2008 *Microsc. Res. Tech.* **71** 35–41
- [7] Flora F et al 2019 *J. Instrum.* **14** C10006
- [8] Mabey P, Albertazzi B, Michel T, Rigon G, Makarov S, Ozaki N, Matsuoka T, Pikuz S, Pikuz T and Koenig M 2019 *Rev. Sci. Instrum.* **90** 063702
- [9] Bonfigli F et al 2019 *Proc. SPIE.* **11035** 110350N
- [10] Vincenti M A et al 2023 *J. Instrum.* **18** C04012
- [11] Vincenti M A et al 2023 *ECS J. Solid State Sci. Technol.* **12** 066008
- [12] Fowler W B 1968 *Physics of Color Centers* (Academic)
- [13] Nahum J 1967 *Phys. Rev.* **158** 814
- [14] Massillon-JL G, Johnston C S N and Kohanoff J 2019 *J. Phys.: Condens. Matter* **16** 025502
- [15] Seitz F 1954 *Rev. Mod. Phys.* **26** 7
- [16] Baldacchini G, Cremona M, Montereali R M, Grassano U M and Kalinov V 1993 *Defects in Insulating Materials* ed O Kanert and J M Spaeth (World Scientific) pp 1103–5
- [17] Dexter D L, Klick C C and Russel G A 1955 *Phys. Rev.* **100** 603
- [18] Bartram R H and Stoneham A M 1975 *Solid State Commun.* **17** 1593–8
- [19] Nahum J and Wiegand D A 1967 *Phys. Rev.* **154** 817
- [20] Ter-Mikirtychev V V and Tsuboi T T 1997 *Can. J. Phys.* **75** 813
- [21] Baldacchini G, de Nicola E, Montereali R M, Scacco A and Kalinov V 2000 *J. Phys. Chem. Solids* **61** 21
- [22] Henke B L, Gullikson E M and Davis J C 1993 *At. Data Nucl. Data Tables* **54** 181–342
- [23] Perez A, Balanzat E and Dural J 1990 *Phys. Rev. B* **41** 3943
- [24] Agulló-López F and Jaque F 1973 *J. Phys. Chem. Solids* **34** 1949
- [25] Bonfigli F, Botti S, Cecilia A, Montereali R M, Nichelatti E, Nigro V, Piccinini M and Vincenti M A 2021 *Condens. Matter* **26** 37